

Towards a Pixel TPC part II: performance of a 32 chip GridPix detector

M. van Beuzekom^a, Y. Bilevych^b, K. Desch^b, S. van Doesburg^a,
H. van der Graaf^a, F. Hartjes^a, J. Kaminski^b, P.M. Kluit^a, N. van der Kolk^a,
C. Ligtenberg^a, G. Raven^a, J. Timmermans^a

^a*Nikhef, Science Park 105, 1098 XG Amsterdam, The Netherlands*

^b*Physikalisches Institut, University of Bonn, Nussallee 12, 53115 Bonn,
Germany*

Abstract

A Time Projection Chamber (TPC) module with 32 GridPix chips was constructed and the performance was measured using data taken in a test beam at DESY in 2021. The analysed data were taken at electron beam momenta of 5 and 6 GeV/c and at magnetic fields of 0 and 1 Tesla(T). Part I of the paper has described the construction, setup and tracking results.

The dE/dx or dN/dx resolution for electrons in the 1 T data for a 1 m track with 60% coverage was measured to be 3.6% for the dE/dx truncation method and 2.9% for the template fit method.

The single electron efficiency at high hit rates was studied. For hit rates up 1.4 kHz per chip a reduction of at most 0.6% in the relative efficiency was measured.

Hit bursts due to highly ionizing particles were characterized.

The resolution in the precision plane as a function of the incident track angle was measured in the $B = 1$ T data using circular tracks. The resolution in the precision plane is - as expected - independent of the incident angle ϕ within an uncertainty of 16 μm .

The projected particle identification performance of a GridPix Pixel TPC in ILD was presented using the $B = 1$ T test beam results for the measured electron resolution. The expected pion-kaon separation for momenta in the range of 2.5-45 GeV/c at $\cos\theta = 0$ is more than 5.5(4.5) σ for the template fit

30 (dE/dx truncation) method.

31 *Keywords:* Micromegas, gaseous pixel detector, micro-pattern gaseous
32 detector, Timepix, GridPix, pixel time projection chamber

33 1. Introduction

34 As a step towards a Pixel Time Projection Chamber for a future collider ex-
35 periment [1], [2], a module consisting of 32 GridPix chips based on the Timepix3
36 chip was constructed. The GridPix chips have a very fine granularity of 55×55
37 μm^2 and a high efficiency to detect single ionisation electrons.

38 The 32 GridPix chip module was put in a test beam at DESY and comple-
39 mented with two sets of Mimosas26 silicon detector planes. The analysed data
40 were taken at electron beam momenta of 5 and 6 GeV/c and at magnetic fields
41 of 0 and 1 T.

42 A description of the construction of the GridPix TPC module, the test beam
43 setup and data taking conditions can be found in part I of our paper [3]. The
44 paper explains the track reconstruction procedure and the precise TPC tracking
45 results that were obtained.

46 2. Analysis topics

47 In the following sections the analysis results for different topics will be pre-
48 sented. Firstly, the particle identification performance using dE/dx or dN/dx
49 will be measured. Secondly, the single electron efficiency at high hit rates will
50 be determined. Thirdly, the characterisation of large hit bursts caused by highly
51 ionizing particles will be presented. Fourth, the resolution in the precision plane
52 as a function of the incident track angle will be measured. Finally, the projected
53 particle identification performance for a Pixel TPC in the ILD experiment [4]
54 will be presented and discussed.

55 2.1. Particle Identification using dE/dx or dN/dx

56 The distribution of the number of TPC track hits per chip for the $B = 0$ T
57 and for the $B = 1$ T data sets are a starting point for a measurement of the

58 dE/dx or dN/dx performance. As was discussed in part I of the paper [3], the
 59 mean number of hits is measured to be 124 and 89 in the B = 0 T and 1 T data
 60 sets respectively. The most probable values are respectively 87 and 64.

61 In order to measure the track performance of dE/dx or dN/dx , the central
 62 chips - defined in ref [3] - were selected and calibrated to give the same mean
 63 number of hits per chip. By combining the hits associated to the track, a new
 64 1 m long track is formed. The 1 m long track has a coverage of 60% because
 65 inactive regions (chip edges and e.g. guard) are included. By applying different
 66 analysis methods, the dE/dx or dN/dx resolution can be measured from data.

67 The first method rejects large clusters with more than 6 hits in 5 consecutive
 68 pixels. Finally a dE/dx truncation at 90% is performed using samples of 20
 69 pixels; so the 10% largest dE/dx values are removed and dE/dx re-estimated.
 70 This method does not fully exploit the full granularity of the pixel TPC.

71 The second method exploits the distribution of the minimum distance in
 72 the precision plane between consecutive hits. If only single electron clusters
 73 were produced in a gas, one would expect an exponentially falling distance
 74 distribution. Multi-electron clusters will give rise to a peak at low distances that
 75 is smeared out by the transverse diffusion process. The slope of the exponential
 76 distribution is proportional to the dN/dx i.e. the clusters produced by the
 77 electron. The long Landau tail in the dE/dx distribution is coming from the
 78 multi-electron clusters that will peak at low distances.

79 Using a large number of tracks, it is possible to measure from data the
 80 shape of the minimum distance distribution. At distances above 10 pixels the
 81 distribution follows an exponential distribution. At lower distance weights for
 82 the B = 0 T and 1 T data are determined and applied to ensure an exponential
 83 distribution over the whole range. Finally, per 1 m track, a fit to distance
 84 distribution in data is performed with the following template function:

$$N(d_{xy}) = N_0 \text{ weight}(d_{xy}) e^{-\text{slope} d_{xy}}. \quad (1)$$

85 where d_{xy} is the minimum distance in the precision plane (xy). The slope and
 86 N_0 - normalisation - are left free in the per track fit, the weights for the B = 0

Table 1: dE/dx or dN/dx resolution for different methods and data sets

Method	B = 0 T resolution	B = 1 T resolution
-	%	%
1 dE/dx truncation	6.0	3.6
2 template fit	5.4	2.9

87 and 1 T data are fixed using the whole data set.

88 The test beam data provides a dE/dx or dN/dx measurement for electrons.
 89 The data were also used to perform a measurement of the response of a mini-
 90 mum ionising particle (MIP) - here defined as a particle that produced 70% of
 91 the electron dE/dx . By dropping 30% of the hits associated to the track and
 92 applying the two methods, the response of a MIP could be measured and the
 93 linearity of the methods tested.

94 The relative resolution is defined as the r.m.s. of the distribution divided by
 95 the mean and the results are shown in Table 1. The resolution of the B = 1 T
 96 data is about 40% better than the B = 0 T data. This is consistent with the
 97 smaller fluctuations that are present in the distributions of the number of hits
 98 per chip in the B = 1 T data [3]. The template fit method has in the B = 1 T
 99 data a 20% better performance than the dE/dx truncation method. One might
 100 argue that with more diffusion the results from the template fit method will
 101 move more towards the results of the dE/dx truncation method. Note however
 102 that the diffusion contribution to the track resolution in the 1 T data is already
 103 sizeable compared to the pixel size and varies between 85-150 μm .

104 The results for the 1 T data are shown in Figure 1 for electrons and MIPs
 105 for the dE/dx truncation and template fit methods. The linearity - defined as
 106 the mean MIP response divided by the mean electron response divided by 0.7
 107 - was measured to be 1.03 for method 1 and 1.07 for method 2. This value is
 108 slightly different from 1, and can be corrected for by scaling the expected values
 109 for different particles as a function of the measured momentum.

110 The dE/dx or dN/dx result of the 32 chip GridPix detector for electrons

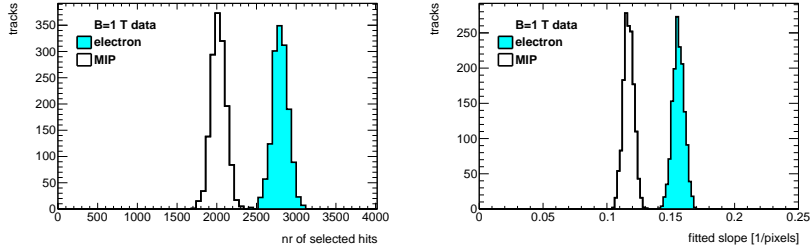


Figure 1: Distribution of the number of selected hits for the dE/dx truncation method (left) and the fitted slope for the template fit method (right) for an electron (light blue shaded) and MIP 1 m long tracks with 60% coverage for the $B = 1$ T data.

111 is impressive. It has currently, the best resolution per meter of track length
 112 of constructed TPCs running at atmospheric pressure - and demonstrates the
 113 particle identification capabilities of a GridPix Pixel TPC.

114 2.2. Single electron efficiency at high hit rates

115 The efficiency of the GridPix device to detect a hit in a high (low) rate
 116 environment is measured comparing the mean time over threshold for low and
 117 high rate runs at B fields of 0 and 1 T. The mean time over threshold is sensitive
 118 to the single electron efficiency of the detector. In order to extract a precise
 119 result, hits associated to TPC tracks were used. The track selection is the same
 120 as the one that was described in the subsection on the particle identification
 121 performance. The analysed runs for the $B = 0$ T data set were runs 6916, 6934
 122 and 6935 and for the $B = 1$ T data set run 6969 and 6983.

123 For each run the mean ToT values were measured for values between 0.15
 124 and $1.4 \mu s$. These cuts were applied to remove the noise and the upper tail of
 125 the distribution.

126 The results for the measured average time over threshold for different runs
 127 and hit rates are summarised in Table 2. ToT1(2) denotes the mean time over
 128 threshold for upper and lower half of the module and Hits1(2) corresponds to
 129 number of recorded raw hits. The mean Rate1(2) was calculated dividing the
 130 total number of raw hits by the total run time. For the $B = 0$ T data, two high

131 rate runs 6934 and 6935 had to be analysed because the beam crossed either
 132 the upper or the lower part of the module and therefore no measurement could
 133 be performed (denoted by -). The statistical uncertainties are - due to the high
 134 statistics - negligible.

135 The relative change in the mean time over threshold for the $B = 0$ data is
 136 -1.2% (upper) and -0.3% (lower). In this case the rate goes up to 8.5 kHz for 6
 137 chips or 1.4 kHz per chip. The relative change in the mean time over threshold
 138 for the $B = 1$ T data is $+1\%$ (upper) and $+1.7\%$ (lower) The rate goes up to 5
 139 kHz for 6 chips or 1.2 kHz per chip.

140 The relative change in the mean time over thresholds $\delta\text{ToT}/\text{ToT}$ can be
 141 related to the relative change in the single electron efficiency $\delta\epsilon/\epsilon$ by:

$$\delta\text{ToT}/\text{ToT} = d \delta\epsilon/\epsilon. \quad (2)$$

142 The derivative d is about 0.5 at the mean working point of $\text{ToT}=0.65 \mu\text{s}$ and is
 143 determined from the measured efficiency- ToT curve in [2].

144 This means that the relative efficiency is stable at the level of $+0.9\%$ ($B = 1$
 145 T) and -0.6% ($B = 0$ T) for hit rates up to 1.2 (1.4) kHz per chip. To conclude,
 146 running at hit rates up 1.4 kHz per chip gives a reduction of at most 0.6% in
 147 the relative efficiency.

Table 2: Mean time of threshold and rates for different runs

run	B	ToT1	ToT2	triggers	run time	Hits1	Hits2	trig rate	Rate1	Rate2
	T	μs	μs	10^3	10^3s	10^6	10^6	Hz	hits/s	hits/s
6916	0	0.628	0.653	16.8	23.2	6.25	13.1	0.72	269	565
6934	0	-	0.651	73.4	2.41	-	20.5	30.4	-	8479
6935	0	0.620	-	7.39	2.41	6.95	-	30.6	2878	-
6969	1	0.650	0.666	7.94	13.8	1.93	2.16	0.57	139	156
6983	1	0.657	0.678	6.79	2.83	11.6	14.1	24.1	4110	4986

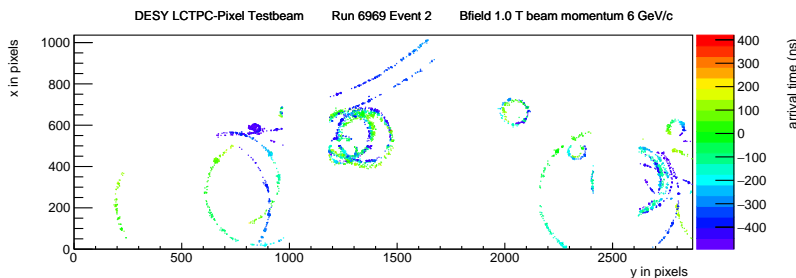


Figure 2: An event display for run 6969 event 2 in a $B = 1$ T field. The hits are shown in the xy plane in color the time of arrival is shown.

148 2.3. Characterisation of hit bursts

149 In event displays hit burst caused by highly ionizing particles (e.g. alpha
 150 particles or delta electrons) can be observed. An example event in run 6969
 151 with $B = 1$ T field is shown in figure 2. A large variety of hit patterns can be
 152 observed: large radii (open) circles from energetic particles, smaller size radius
 153 circles, curlers and more confined bursts.

154 A Pixel TPC is well suited to study and characterize these typical hit bursts.
 155 A pixel TPC also allows to improve the high momentum tracking by removing
 156 these bursts.

157 To study the hit bursts the data of run 6969 $B = 1$ T was analysed. Bursts
 158 were selected with more than 100 hits in a radius of 50 pixels around the burst
 159 center within a time window of 200 ns around the mean time. The mean position
 160 in xy and the mean time of the burst were iteratively estimated. The bursts
 161 were characterized by the number of associated hits, the radius in which 90% of
 162 the hits are found (radius90) and the time in which 90% of the hits are detected
 163 (time90). The stacked distributions for the radius90 and time90 variables for
 164 different burst sizes are shown in Figure 3.

165 It is clear that the radius90 and time90 distributions broaden as a function
 166 of the number of hits. In particular the time90 distribution develops a long tail
 167 for high number of hits. Note that hits that end up on the same pixel within the
 168 TimePix3 pixel dead time of 475 ns will not be recorded, so part of the core of

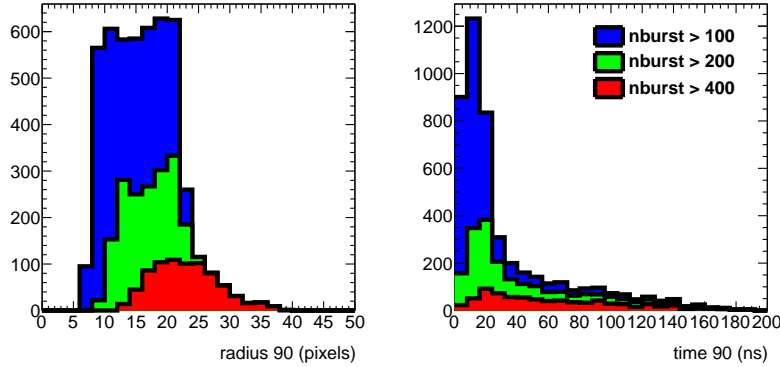


Figure 3: The stacked distributions for radius90 and time90 for burst with more than 100 (blue), 200 (green) and 400 (red) hits for run 6969 in a $B = 1$ T field.

169 the burst might stay undetected. Still the detector is able to record hit bursts
 170 of at most 7854 hits in a 50 pixel radius. The largest hit burst in run 6969 had
 171 3180 hits.

172 For high momentum tracking it is important to cut tightly on the track
 173 residuals in xy and z . In particular the cut in z reduces the impact of bursts
 174 in the $B = 1$ T data. One could in addition run a burst finding algorithm
 175 and down weight the hits associated to burst and the selected track. This will
 176 remove biases and improve the track parameter estimation.

177 *2.4. Resolution study*

178 The resolution in the precision plane as a function of the incident track angle
 179 will be measured in the $B = 1$ T data set. For a pad based readout system the
 180 resolution has a strong dependence on the incident angle see e.g. reference [5].
 181 The resolution is minimal if the incident track angle is parallel to the strip
 182 direction. This is due to the geometrical strip layout.

183 For a GridPix pixel TPC - with squared pixels - the resolution is expected
 184 to be independent of the incident angle. In order to test experimentally this
 185 hypothesis, circular tracks were selected. Examples of circular tracks can be
 186 observed in the event display shown in Figure 2. Using these circles, the incident

187 ϕ angle of the individual hits (with respect to the y axis) can be probed over a
188 large range and the resolution in xy measured.

189 A dedicated pattern recognition program was written to find and fit multiple
190 circles in an event. To find circles large clusters were down weighted and hits
191 within 15 pixels (in xy) of the chip edge were removed. In the circle fit, the
192 resolution in xy was assumed to be 4 pixels and in z of 1 mm. Outlier hits at
193 more than 2.5 standard deviation were iteratively rejected. For the selection of
194 circles it was required that the fit χ_{xy}^2/dof and χ_z^2/dof was less than 5. Finally,
195 the radius of the circle had to be larger than 50 pixels (corresponding to a
196 momentum cut of 0.4 MeV/c), at least 20 hits should lie on the circle. The
197 ϕ ranges from $\pi/4$ to $7\pi/4$ and total ϕ span of the selected hits on the circle
198 should be at least 1 rad.

199 The selected data set has 973 circles, with a mean radius of 155 pixels and a
200 mean number of hits of 194. Because the resolution depends on the radius and
201 small radii span a large phi range, the data was re-weighted as a function of the
202 radius. Finally, the resolution in xy was extracted - using a Gaussian fit in the
203 range of $\pm 2\sigma$ around the centre. The fitted resolution in xy as a function of the
204 ϕ incident angle of the hits on the circle is shown in Figure 4.

205 A curve was fitted to the data using the following expression:

$$\sigma_{xy} = \sigma_0 + \sigma_1 \cos \phi, \quad (3)$$

206 where σ_0 and σ_1 were left free. The fit result yielded $\sigma_0 = 0.241$ mm and σ_1
207 $= 0.016$ mm and describes the modulation observed in the data.

208 It can therefore be concluded that the resolution in the precision plane is
209 independent of the incident angle ϕ within an uncertainty of 16 μm .

210 2.5. Projected particle identification performance

211 The projected particle identification performance for a Pixel TPC in ILD will
212 be presented. The TPC of ILD has an inner radius of 329 mm, an outer radius
213 of 1770 mm and a half length of 2350 mm. The electron resolution from the test
214 beam for momenta of 5-6 GeV/c is 2.9% for the template fit and 3.6% for the

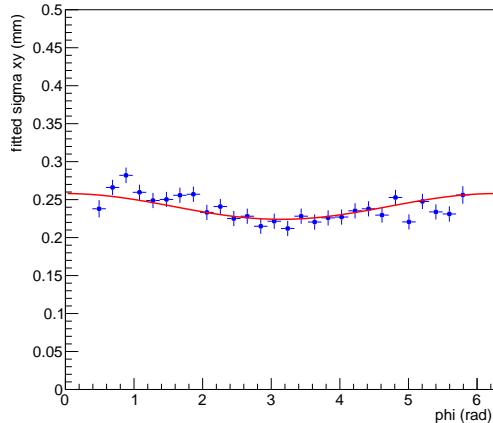


Figure 4: The fitted resolution in xy as a function of the ϕ incident angle of the hits on the circle. The fitted curved in red is given in Eq. 3.

215 dE/dx truncation method at $B = 1$ T for a 1 m long tracks with 60% coverage.
 216 In the ILD TPC this will correspond to an expected electron resolution of 2.4%
 217 (fit) and 3% (truncation) at polar a angles of $\theta = \pi/2$ ($\cos \theta = 0$) and a track
 218 length ($tlength_0$) of 1441 mm. Depending on the B field value (3.5 T - foreseen
 219 at ILC - or e.g. 2 T), the transverse diffusion value in the T2K gas will be
 220 similar or worse than the test beam situation. The resolution for a GridPix
 221 TPC in ILD will therefore lie between 2.4 and 3% at $\cos \theta = 0$. The resolution
 222 for different particles can be written as:

$$\sigma = \sigma_e \sqrt{tlength_0 E_e} / \sqrt{tlength E_i}, \quad (4)$$

223 where $tlength$ is the track length and E_i is the expected energy loss for particle
 224 i (electron = e , muon = μ , pion = π , kaon = K , proton = p). Clearly, the best
 225 resolution will be reached for the largest track length that corresponds in ILD
 226 to $\cos \theta = 0.85$.

227 The ILD parametrisations for the energy loss for different particles as a
 228 function of the momentum were used [6]. They are based on full simulations of
 229 the ILD TPC operated with a T2K gas and running at atmospheric pressure.

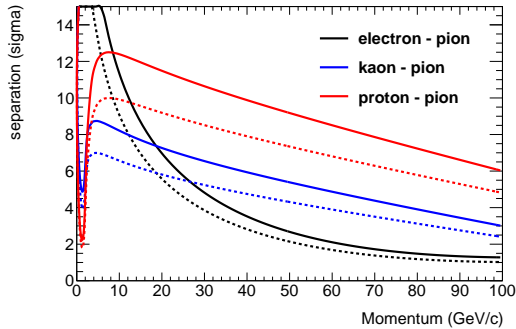


Figure 5: The projected separation for a GridPix TPC in ILD for electrons, kaons and protons w.r.t. pions at $\cos\theta = 0$. The continuous line corresponds to an electron resolution of 2.4% and the dashed to 3%.

230 The separation in numbers of standard deviations w.r.t. the π hypothesis for
 231 the e , K and p is defined as:

$$\text{separation} = |E_i - E_\pi|/\sigma_\pi, \quad (5)$$

232 In Figure 5, the separation of electrons, kaons and protons w.r.t. pions is
 233 shown as a function of the momentum of the particle for projected ILD electron
 234 resolutions of 2.4 and 3% at $\cos\theta = 0$.

235 The expected pion-kaon separation for momenta in the range of 2.5-45 GeV/c
 236 at $\cos\theta = 0$ is more than 5.5(4.5) σ for the two resolution scenarios. At a mo-
 237 mentum of 100 GeV/c the separation is still 3.0(2.0) σ . Protons can be separated
 238 from pions for momenta in the range of 2.5-100 GeV/c with more than 6.0(4.8) σ .

239 It is clear from the above that a GridPix Pixel TPC in ILD will provide very
 240 powerful particle identification.

241 3. Conclusion and outlook

242 A Time Projection Chamber (TPC) module with 32 GridPix chips was con-
 243 structed and the performance was measured using data taken in a test beam at
 244 DESY in 2021. The analysed data were taken at electron beam momenta of 5
 245 and 6 GeV/c and at magnetic fields of 0 and 1 T.

246 The precise tracking results for the module were presented in part I of the
247 paper [3].

248 The dE/dx or dN/dx resolution for electrons of momenta 5 and 6 GeV/c
249 in the 1 T data for a 1 m track with 60% coverage was measured to be 3.6%
250 for the dE/dx truncation method and 2.9% for the template fit method. This
251 result is impressive. It is currently, the best resolution per meter of track length
252 of constructed TPCs running at atmospheric pressure.

253 The single electron efficiency at high hit rates was studied. For hit rates
254 up 1.4 kHz per chip a reduction of at most 0.6% in the relative efficiency was
255 measured.

256 Hit bursts due to highly ionizing particles were characterized showing the
257 pattern recognition capabilities of a GridPix Pixel TPC.

258 The resolution in the precision plane as a function of the incident track angle
259 was measured in the $B = 1$ T data using circular tracks. It was demonstrated
260 that the resolution in the precision plane is - as expected - independent of the
261 incident angle ϕ within an uncertainty of 16 μm .

262 The projected particle identification performance of a GridPix Pixel TPC
263 in ILD was presented using the $B = 1$ T test beam results for the measured
264 electron resolution. The expected pion-kaon separation for momenta in the
265 range of 2.5-45 GeV/c at $\cos\theta = 0$ is more than 5.5 (4.5) σ for the template fit
266 (dE/dx truncation) method.

267 It is clear that a GridPix Pixel TPC in ILD will provide very powerful particle
268 identification. At the CEPC collider a Pixel TPC is proposed, because of the
269 precise tracking and particle identification capabilities. The GridPix detector
270 will be further tested and developed for a TPC that will be installed in a heavy
271 ion experiment at the EIC. In the DRD1 collaboration at CERN a GridPix
272 Pixel TPC is also part of the research program.

273 **Acknowledgments**

274 This research was funded by the Netherlands Organisation for Scientific Re-
275 search NWO. The authors want to thank the support of the mechanical and
276 electronics departments at Nikhef and the detector laboratory in Bonn. The
277 measurements leading to these results have been performed at the Test Beam
278 Facility at DESY Hamburg (Germany), a member of the Helmholtz Association
279 (HGF).

280 **References**

- 281 [1] M. Lupberger, Y. Bilevych, H. Blank, D. Danilov, K. Desch, A. Hamann,
282 J. Kaminski, W. Ockenfels, J. Tomtschak, S. Zigann-Wack, Toward the
283 Pixel-TPC: Construction and Operation of a Large Area GridPix Detector,
284 IEEE Trans. Nucl. Sci. 64 (5) (2017) 1159–1167. doi:10.1109/TNS.2017.
285 2689244.
- 286 [2] C. Ligtenberg, A GridPix TPC readout for the ILD experiment at the
287 future International Linear Collider, Ph.D. thesis, Free University of
288 Amsterdam (2021).
289 URL [https://www.nikhef.nl/pub/services/biblio/theses_pdf/
290 thesis_C_Ligtenberg.pdf](https://www.nikhef.nl/pub/services/biblio/theses_pdf/thesis_C_Ligtenberg.pdf)
- 291 [3] M. van Beuzekom, et al., Towards a Pixel TPC part I: construction and
292 test of a 32 chip GridPix detector, submitted to Nucl. Instrum. Meth. A.
- 293 [4] T. Behnke, J. E. Brau et al., eds. The International Linear Collider. Techni-
294 cal Design Report. Vol. 4: Detectors. Linear Collider Collaboration, 2013.
295 arXiv: 1306.6329. doi:10.48550/arXiv.1306.6329.
296 URL <https://www.linearcollider.org/>
- 297 [5] LCTPC Collaboration, David Attié et al., A Time Projection Chamber
298 with GEM-Based Readout, Nuclear Instruments and Methods in Physics

299 Research. Section A: Accelerators, Spectrometers, Detectors and Asso-
300 ciated Equipment 856, 1 (2017), 109–118. arXiv:1604.00935v1, doi:
301 10.1016/j.nima.2016.11.002.

302 [6] iLCSoft, Linear Collider Software,
303 URL [https://github.com/iLCSoft/MarlinReco/blob/master/](https://github.com/iLCSoft/MarlinReco/blob/master/Analysis/PIDTools/)
304 [Analysis/PIDTools/](https://github.com/iLCSoft/MarlinReco/blob/master/Analysis/PIDTools/), based on version v02-02-01.